

Na₅Sn₁₃: A New Zintl Phase with a Complex Network Structure Constructed from Tin Pentagons

J. T. Vaughey and John D. Corbett*

Ames Laboratory¹ and Department of Chemistry, Iowa State University, Ames, Iowa 50011

Received March 18, 1997[⊗]

The compound Na₅Sn₁₃ forms in the sodium–tin system in high yield following prolonged reaction of a quenched mixture at 280 °C in a Ta container. The compound exhibits a complex three-dimensional structure (29 independent atoms) built mainly of 4-bonded tin atoms in interbonded pentagons (orthorhombic, space group *Cmcm* (No. 63); $a = 8.979(1)$ Å, $b = 19.448(6)$ Å, $c = 50.43(2)$ Å, $Z = 16$). According to Zintl–Klemm electron-counting formalisms, the compound has a closed-shell electronic configuration with the number of 3-bonded Sn[−] equal to the number of sodium cations. Property measurements show that the compound is diamagnetic.

Introduction

The recent observation of record thermoelectric properties in the skutterite type phase LaFe₃Sb₁₂² has increased interest in main-group framework structures. The need to better understand what factors are important in the formation of such framework structures has led us in recent years to study these types of materials. Recently we reported on the new compound NaGaSn₂, an all-tetrahedral Zintl phase possessing large one-dimensional channels reminiscent of known microporous materials.³ As a continuation of these goals, we have started looking for structures with mixtures of 3- and 4-bonded constituents in new frameworks. Using Zintl's rules as a predictive tool, we have chosen to study the tin-rich side of the sodium–tin system where a mixture of the these bonding geometries would be postulated.

The sodium–tin phase diagram was first reported in 1928 by Hume-Rothery.⁴ Of the nine compounds reported to date,⁵ only those on the sodium-rich side of the phase diagram have been identified and studied in detail,⁶ while the four compounds deduced on the tin-rich side have received little attention. Several presumably related framework compounds were recently identified in other alkali-metal–tin systems. One, A₈Sn₄₄ for A = K or Rb, has a sodalite or clathrate-I type structure in which a random distribution of tin vacancies on one site in an all-tetrahedral framework provide the charge compensation necessary for it to be a Zintl phase.⁷ (A wide variety of isoelectronic and isotypic ternary analogues have also been characterized, e.g., K₈Ga₈Sn₃₈.⁸) Another K₈Sn₂₅ phase represents a new structural type as it is built from rare pentagonal-faced dodecahedra of tin that share faces,⁷ and the structure again meets the requirements of a Zintl phase. These com-

pounds as well as two with oligomeric tin components, formally Sn₂^{6−}, Sn₅^{12−}, and Sn₆^{14−},^{9,10} highlight the extent to which bonding in tin compounds can vary to meet the Zintl–Klemm criteria of octet (closed-shell) bonding of the p-block elements.¹¹ This has encouraged us to search for other examples, and this paper reports another such product Na₅Sn₁₃, which was previously labeled as “NaSn₃” in the phase diagram.

Experimental Section

Syntheses. The general techniques employed were as previously described.¹² All materials were handled only in a N₂-filled glovebox with a moisture level below 0.1 ppm (volume). An initial sample of composition “NaSn₃” was prepared by weighing stoichiometric amounts of the elements sodium (Alfa, 99.9+%) and tin (Johnson-Matthey, 99.9999%) into a tantalum tube, one end of which had been previously welded. The other end of the tube was then crimped, welded, and placed inside a silica jacket that was evacuated and sealed. The mixture was heated to 800 °C, held for 1 day, quenched, then annealed at 280 °C over a 3-week period, and quenched into a water bath. This cycle was chosen in accordance with the phase relationships proposed for the composition NaSn₃.⁴

Analysis of the silvery sample by Guinier powder diffraction methods revealed only Sn and the lines of the phase later identified as Na₅Sn₁₃. Once the unit cell and structure had been established by single-crystal X-ray diffraction methods, the lattice constants were refined with the aid of 33 indexed lines from the powder pattern, Si as an internal standard, and a nonlinear least-squares method. The powder pattern calculated for the new phase agreed very well with that observed for this sample. The compound was obtained in high yield (>95%) by direct reaction of the elements in the correct stoichiometry in a manner similar to that described above, except the quenched sample was annealed at 280 °C for 10 weeks. The long annealing time appears necessary to allow for complete diffusion of the elements into a homogeneous material and for crystal growth at such low temperatures. Reactions attempted under the same conditions that were loaded tin-rich showed a mixture of Na₅Sn₁₃ and elemental tin, while sodium-richer reactions (e.g., Na₆Sn₁₃) produced a nonequilibrium mixture of Na₅Sn₁₃, unreacted tin, and an unidentified phase that, according to the phase diagram, is labeled as NaSn₂ and has an unknown structure. Lattice constants from indexed powder patterns of samples in which Na₅Sn₁₃ was the dominant phase are given in Table 1. These show little variation with composition, indicative of a line phase.

[⊗] Abstract published in *Advance ACS Abstracts*, September 1, 1997.

- (1) This research was supported by the Office of the Basic Energy Sciences, Materials Science Division, U.S. Department of Energy. Ames Laboratory is operated for DOE by Iowa State University under Contract No. W-7405-Eng-82.
- (2) Sales, B. C.; Mandrus, D.; Williams, R. K. *Science* **1996**, *272*, 1325.
- (3) Vaughey, J. T.; Corbett, J. D. *J. Am. Chem. Soc.* **1996**, *118*, 12098.
- (4) Hume-Rothery, W. *J. Chem. Soc.* **1928**, *131*, 947.
- (5) *Binary Alloy Phase Diagrams*; 2nd ed.; Massalski, T. B., Ed.; ASM International: Materials Park, OH, 1990; Vol. 3, p 2734.
- (6) (a) Müller, W.; Volk, K. Z. *Naturforsch.* **1977**, *32B*, 709. (b) Müller, W.; Volk, K. Z. *Naturforsch.* **1978**, *33B*, 275. (c) Guerin, F.; Richeson, D. *J. Chem. Soc., Chem Commun.* **1994**, 2213.
- (7) Zhao, J.-T.; Corbett, J. D. *Inorg. Chem.* **1994**, *35*, 5721.
- (8) Kröner, R. Doctoral Dissertation, University of Stuttgart, 1989. von Schnering, H.-G. Private communication.

(9) Ganguli, A.; Guloy, A. M.; Leon-Escamilla, E. A.; Corbett, J. D. *Inorg. Chem.* **1993**, *32*, 4349.

(10) Leon-Escamilla, E. A.; Corbett, J. D. To be published.

(11) Kauzlarich, S., Ed. *Structure and Bonding of Zintl Phases and Ions*; VCH Publishers: Boca Raton, FL, 1996.

(12) Zhao, J.-T.; Corbett, J. D. *Inorg. Chem.* **1995**, *34*, 378.

Table 1. Lattice Constants from Indexed Powder Patterns for Na₅Sn₁₃^a

compn	no. of lines	<i>a</i> , Å	<i>b</i> , Å	<i>c</i> , Å	<i>V</i> , Å ³
"Na ₆ Sn ₁₃ "	24	8.981(3)	19.465(8)	50.50(2)	8828(2)
Na ₅ Sn ₁₃	31	8.983(3)	19.446(8)	50.53(1)	8826(1)
Na ₅ Sn ₁₃ ^b	33	8.979(1)	19.448(6)	50.43(2)	8806(2)
Na ₅ Sn ₁₃	18	8.974(2)	19.450(6)	50.48(2)	8811(2)
"Na ₅ Sn ₁₅ "	17	8.974(3)	19.479(9)	50.43(2)	8815(2)

^a Least-squares results from Guinier powder pattern data with Si as internal standard; $\lambda = 1.540\ 562\ \text{\AA}$, 22 °C. ^b Data crystal.

Table 2. Selected Data Collection and Refinement Parameters for Na₅Sn₁₃

fw	1658.06	rel transm	0.335–1.00
crystal system ^a	orthorhombic	coeff range	
space group, <i>Z</i>	<i>Cmcm</i> (No. 63), 16	residuals	6.7/8.2
<i>d</i> _{calc} g/cm ³	5.022	<i>R/R</i> _w , ^b (%)	

^a Lattice dimensions are given in Table 1. ^b $R = \sum ||F_o| - |F_c|| / \sum |F_o|$; $R_w = [\sum w(|F_o| - |F_c|)^2 / \sum w F_o^2]^{1/2}$; $w = \sigma_F^{-2}$.

Table 3. Refined Atomic Positions and Isotropic-Equivalent Thermal Parameters for Na₅Sn₁₃

atom	Wyckoff position	<i>x</i>	<i>y</i>	<i>z</i>	<i>B</i> (eq), ^a Å ²
Sn1	8 <i>f</i>	0	0.4023(2)	0.44909(7)	1.5(2)
Sn2	8 <i>f</i>	1/2	0.5008(2)	0.34764(7)	1.3(2)
Sn3 ^b	8 <i>f</i>	1/2	0.3701(2)	0.41908(7)	1.5(2)
Sn4 ^b	8 <i>f</i>	0	0.5832(2)	0.30908(7)	1.3(2)
Sn5 ^b	8 <i>f</i>	1/2	0.3609(2)	0.33038(7)	1.5(2)
Sn6 ^b	8 <i>f</i>	0	0.2802(2)	0.41811(7)	1.4(2)
Sn7 ^b	8 <i>f</i>	1/2	0.2718(2)	0.46127(7)	1.7(2)
Sn8 ^b	8 <i>f</i>	0	0.3414(2)	0.32173(7)	1.2(2)
Sn9	16 <i>h</i>	0.2668(4)	0.4689(1)	0.43122(5)	1.4(1)
Sn10	8 <i>f</i>	0	0.4745(2)	0.34664(6)	1.3(2)
Sn11	16 <i>h</i>	0.2992(5)	0.5848(1)	0.46863(5)	1.8(1)
Sn12 ^b	8 <i>f</i>	1/2	0.5936(2)	0.30301(7)	1.5(2)
Sn13 ^b	16 <i>h</i>	0.1612(4)	0.6722(1)	0.37787(5)	1.6(1)
Sn14	16 <i>h</i>	0.2368(4)	0.5277(1)	0.37812(4)	1.3(1)
Sn15	16 <i>h</i>	-0.2464(4)	0.5291(1)	0.27909(4)	1.2(1)
Sn16	8 <i>f</i>	0	0.4285(2)	0.50624(7)	2.4(2)
Sn17	16 <i>h</i>	0.2641(4)	0.2028(1)	0.43334(5)	1.6(1)
Sn18	16 <i>h</i>	0.2644(4)	0.3833(1)	0.29340(4)	1.3(1)
Sn19 ^b	8 <i>g</i>	0.3345(6)	0.2901(2)	1/4	1.4(2)
Na1	4 <i>c</i>	0	0.416(2)	1/4	3(2)
Na2	4 <i>c</i>	1/2	0.444(2)	1/4	3(2)
Na3	8 <i>f</i>	1/2	0.431(1)	0.4795(4)	3(1)
Na4	8 <i>f</i>	0	0.577(1)	0.4254(4)	2(1)
Na5	8 <i>f</i>	0	0.198(1)	0.3573(5)	3(1)
Na6	8 <i>g</i>	0	0.357(1)	3/4	2(2)
Na7	8 <i>f</i>	0	0.095(1)	0.0859(5)	3(1)
Na8	16 <i>h</i>	0.257(3)	0.1579(8)	0.6247(3)	4(1)
Na9	16 <i>h</i>	0.285(3)	0.2166(8)	0.1872(3)	3(1)
Na10	8 <i>g</i>	0	0.198(3)	1/4	7(4)

^a $B_{\text{eq}} = (8\pi^2/3) \sum_i \sum_j U_{ij} a_i^* a_j^* \vec{a}_i \vec{a}_j$. ^b 3-bonded Sn atoms.

Structural Studies. The single crystals of the compound used in the X-ray diffraction measurements were initially isolated from reactions loaded as "NaSn₃". Several were sealed into thin-walled capillary tubes, and Laue photographs were used to determine which crystal was most suitable for structural determination. Diffraction data were collected at room temperature on an Enraf-Nonius CAD4 diffractometer with Mo K α radiation. Cell constants and an orientation matrix for data collection were determined from a least-squares refinement of the setting angles of 25 centered reflections. In total, 8059 reflections were measured for the *C*-centered cell in the $\pm h, k, l$ octants up to $2\theta = 50^\circ$; of these, 4552 reflections were observed ($I/\sigma(I) > 3$). (A previous data set collected on the same crystal without the *C*-centering restrictions showed no violations.) The systematic absences indicated either space group *Cmcm* (No. 63) or *Cmc*₂ (No. 36). Intensity statistics indicated a centrosymmetric space group, and the refinement proceeded successfully in *Cmcm*. The structure was solved by direct methods with the aid of the program package TEXSAN.¹³ Anomalous dispersion

Table 4. Bond Distances in Na₅Sn₁₃^a

atom	atom	dist, Å	atom	atom	dist, Å
Sn1	Sn6	2.843(5)	Sn15	Sn4	2.879(4)
	Sn9	2.869(4) × 2		Sn12	2.865(4)
	Sn16	2.927(5)		Sn15	2.934(4)
Sn2	Sn5	2.857(5)		Sn18	2.931(3)
	Sn12	2.885(5)		Na1	3.45(2)
	Sn14	2.867(2) × 2		Na2	3.17(2)
Sn3	Sn7	2.861(5)		Na6	3.46(2)
	Sn9	2.907(4) × 2	Sn16	Sn1	2.927(5)
	Na3	3.27(2)		Sn11	2.982(4) × 2
	Na8	3.24(2) × 2		Sn16	2.851(8)
Sn4	Sn10	2.837(5)		Na4	3.45(2)
	Sn15	2.879(4) × 2	Sn17	Sn6	2.911(4)
	Na6	3.20(1)		Sn7	2.875(4)
	Na9	3.24(2) × 2		Sn11	2.959(3)
Sn5	Sn2	2.857(5)		Sn13	2.938(4)
	Sn18	2.853(4) × 2		Na4	3.26(2)
	Na8	3.25(2) × 2		Na7	3.31(2)
	Na9	3.52(2) × 2	Sn18	Sn5	2.853(4)
Sn6	Sn1	2.843(5)		Sn8	2.888(4)
	Sn17	2.911(4) × 2		Sn15	2.931(3)
	Na5	3.46(3)		Sn19	2.910(3)
	Na8	3.30(2) × 2		Na1	3.292(8)
Sn7	Sn3	2.861(5)		Na2	3.26(1)
	Sn17	2.875(4) × 2		Na9	3.39(2)
	Na3	3.23(2)	Sn19	Sn18	2.910(3) × 2
Sn8	Sn10	2.877(5)		Sn19	2.97(1)
	Sn18	2.888(4) × 2		Na2	3.34(3)
	Na5	3.32(2)		Na6	3.22(2)
	Na8	3.47(2) × 2		Na9	3.50(2) × 2
	Na9	3.56(2)		Na10	3.49(3)
Sn9	Sn1	2.869(4)	Na1	Sn15	3.45(2) × 4
	Sn3	2.907(4)		Sn18	3.292(8) × 4
	Sn11	2.954(3)	Na2	Sn15	3.17(2) × 4
	Sn14	2.924(3)		Sn18	3.26(1) × 4
	Na3	3.30(2)	Na3	Sn19	3.34(3) × 2
	Na4	3.20(1)		Sn3	3.27(2)
	Na7	3.34(2)		Sn7	3.23(2)
Sn10	Sn4	2.837(5)		Sn9	3.30(2) × 2
	Sn8	2.877(5)		Sn11	3.53(2) × 2
	Sn14	2.848(4) × 2		Sn12	3.18(2) × 2
Sn11	Sn9	2.954(3)	Na4	Sn9	3.20(1) × 2
	Sn16	2.982(4)		Sn11	3.46(1) × 2
	Sn17	2.959(3)		Sn13	3.36(2) × 2
	Sn11	3.606(8)		Sn14	3.34(2) × 2
	Na3	3.18(2)		Sn16	3.45(2)
		3.53(2) × 2		Sn17	3.26(2) × 2
	Na4	3.46(1)	Na5	Sn6	3.46(3)
	Na7	3.29(2)		Sn8	3.32(2)
Sn12	Sn2	2.885(5)		Sn12	3.40(3)
	Sn15	2.865(4) × 2		Sn13	3.252(9) × 2
	Na5	3.40(3)	Na6	Sn4	3.20(1) × 2
	Na9	3.54(2) × 2		Sn15	3.46(2) × 4
	Na10	3.36(3)		Sn19	3.22(2) × 2
Sn13	Sn13	2.894(7)	Na7	Sn9	3.34(2) × 2
	Sn14	2.892(3)		Sn11	3.29(2) × 2
	Sn17	2.938(4)		Sn14	3.26(2) × 2
	Na4	3.36(2)		Sn17	3.31(2) × 2
	Na5	3.252(9)	Na8	Sn3	3.27(2)
	Na8	3.42(2)		Sn5	3.24(2)
	Na9	3.43(4)		Sn6	3.25(2)
Sn14	Sn2	2.867(4)		Sn8	3.47(2)
	Sn9	2.924(3)		Sn13	3.42(2)
	Sn10	2.848(4)	Na9	Sn4	3.24(2)
	Sn13	2.892(3)		Sn5	3.52(2)
	Na4	3.34(2)		Sn8	3.56(2)
	Na7	3.26(2)		Sn12	3.54(2)
				Sn13	3.43(2)
				Sn18	3.39(2)
				Sn19	3.50(2)
			Na10	Sn12	3.36(3) × 2
				Sn19	3.49(3) × 2

^a The distance cutoff for the data listed is 3.56 Å. The shortest Na–Na separation is 3.38(4) Å.

was taken into account during the refinement. The initial absorption correction was based on five ψ scans, and DIFABS was applied after the isotropic refinement, as recommended by the authors of the program,¹⁴ as an improved absorption correction for the crystal with a

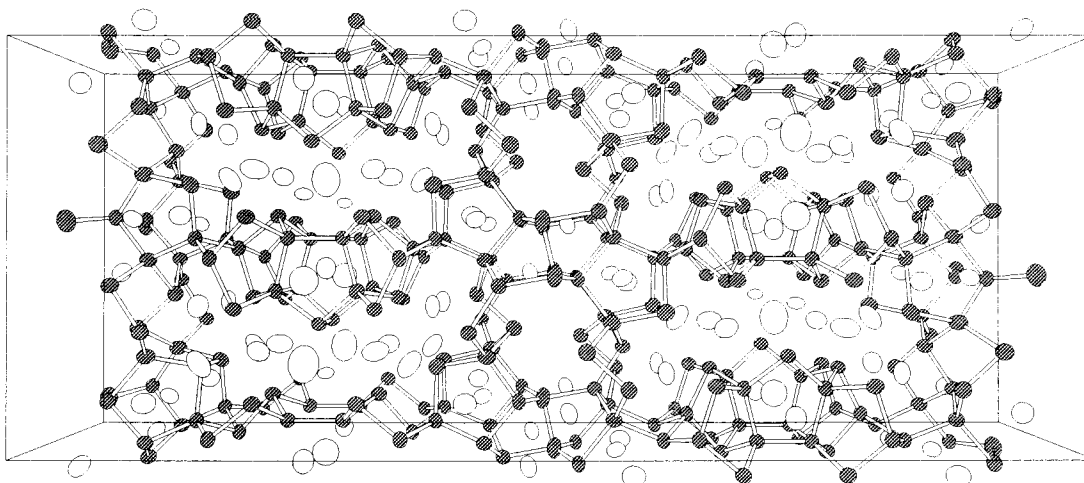


Figure 1. The structure of $\text{Na}_5\text{Sn}_{13}$ looking down the 8.98 \AA a axis. (The long axis is c .) The open spheres are sodium cations, while the darkened spheres represent tin atoms. The thermal ellipsoids are drawn at 98% probability.

5:1 aspect ratio. The data were averaged and reduced to 4325 independent observations ($R_{\text{av}} = 12.1\%$ for $I/\sigma(I) > 3$) of which 2152 were observed. The anisotropic refinement of all atoms resulted in R , R_w values of 6.7, 8.2% at convergence. Summary data are given in Table 2.

The maximum and minimum peaks in the final difference Fourier map were 4.5 e/\AA^3 (3.1 \AA from Sn7) and -3.5 e/\AA^3 . The largest peak is only $\sim 1 \text{ e/\AA}^3$ above the background level and sits only 1.1 \AA from an inversion center. Attempts to refine this as a sodium cation were unsuccessful, giving large isotropic thermal parameters as well as unusually short distances (2.2 \AA) to neighboring cations. The high background is probably a result of the slight peak overlap observed to occur along the long c axis, 50.43 \AA . Long exposure ($> 1 \text{ h}$) axial photographs confirmed the repeat lengths of the two larger axes (b , c) and the expected mirror symmetry. The use of smaller alternative unit cells or lower symmetry orthorhombic or monoclinic space groups failed to produce a reasonable structural refinement. The only faint indication of any problem might be a slight asymmetry of the anisotropic thermal ellipsoid observed for Sn16 ($U_{11}/U_{33} \approx 2.3$). As will be seen, this atom has the three of the longest Sn–Sn bonds in the structure (2.927 \AA , $2.982 \text{ \AA} \times 2$) as well as some of the most divergent angles in its flattened quasi-tetrahedral geometry (87.32° , $100.27^\circ \times 2$, $113.77^\circ \times 2$, 128.62°) owing to its location at the base of the central ring. With its flattened coordination polyhedron and long bonds, the observed slight elongation of its anisotropic thermal ellipsoid toward the central void it borders is not a likely indication of any crystallographic error.

Additional crystallographic data and the anisotropic displacement parameters are given in the Supporting Information. These and the F_o/F_c data are also available from J.D.C.

Properties. Magnetic measurements on 46.6 mg of a single-phase sample were carried out on a Quantum Design MPMS SQUID susceptometer. The sample was loaded into an improved fused-silica susceptibility container in a He-filled glovebox.¹⁵ Measurements were made over $5\text{--}300 \text{ K}$ in a 3 T field. The data were corrected for core diamagnetism and for a small paramagnetic tail evident below $\sim 80 \text{ K}$ with the aid of a simple model $S = 1/2$ spin system as employed by Hendrickson et al. in recent years.¹⁶ The source of this small paramagnetic impurity is unknown, but possible sources include the surface coating that forms between the sample and the Ta container wall (evident in SEM/EDX experiments) or impurities introduced during grinding and handling of the sample in the glovebox.

Extended Hückel calculations on the anion lattice were done using a local variant of the EHMACC program written and modified by R.

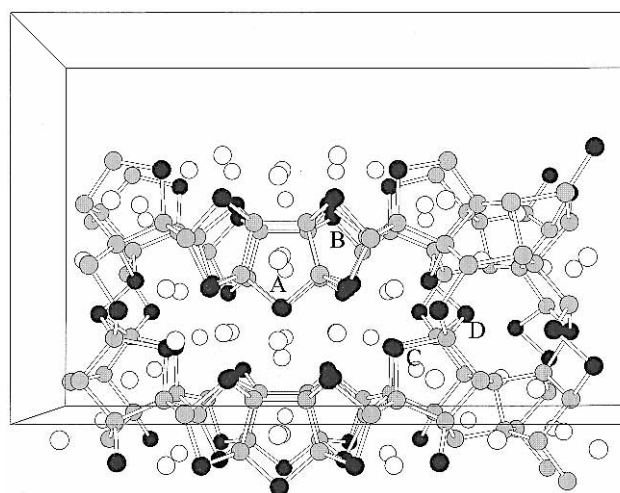


Figure 2. A segment of $\text{Na}_5\text{Sn}_{13}$ viewed along \bar{a} that highlights the approximate repeat unit of the structure shown in Figure 1. The 3-bonded tin atoms are the black circles. The letters A, B, C, D mark the different pieces of the structure described in detail in the text. The columns of A units lie on a vertical mirror plane.

Hoffmann's group at Cornell University. The tin parameters were the default values from the standard tables. Seven well-spaced k -points were used in the calculations.

Results and Discussion

The compound $\text{Na}_5\text{Sn}_{13}$ represents a new structure type in the Zintl chemistry of the group 14 elements,^{11,17} with 19 independent tin and 10 sodium atoms, a surprising complexity for a binary compound. The atom positions and isotropic-equivalent ellipsoid values are listed in Table 3, and the bond distances appear in Table 4. A $[100]$ projection of the contents of about one cell is shown in Figure 1. The main structural components are infinite chains of interconnected clusters built of tin pentagons stacked along the a axis of the compound, labeled "A" in the detail in Figure 2. (A copy of this figure in the Supporting Information includes labels for the atoms.) These pentagons contain four formally neutral and nearly coplanar 4-bonded tin (4b-Sn) atoms and a 3-bonded apex tin atom (black) at the bottom that is formally Sn^- . These central pentagons are connected to each other in two different manners.

(13) TEXSAN, version 6.0; Molecular Structure, Corp.: The Woodlands, TX, 1990.

(14) Walker, N.; Stuart, D. *Acta Crystallogr.* **1983**, A39, 158.

(15) Guloy, A. M.; Corbett, J. D. *Inorg. Chem.* **1996**, 35, 4670.

(16) (a) Jameson, D. L.; Xie, C.-L.; Hendrickson, D. N.; Potenza, J. A.; Schugar, H. J. *J. Am. Chem. Soc.* **1987**, 109, 740. (b) Felthous, T. R.; Dong, T. Y.; Hendrickson, D. N.; Shieh, H. S.; Thompson, M. R. *J. Am. Chem. Soc.* **1986**, 108, 8201.

(17) (a) Zintl, E. *Angew. Chem.* **1939**, 52, 1. (b) Klemm, W.; Busmann, E. *Z. Anorg. Allg. Chem.* **1963**, 319, 297. (c) Schäfer, H. *Annu. Rev. Mater. Chem.* **1985**, 15, 1.

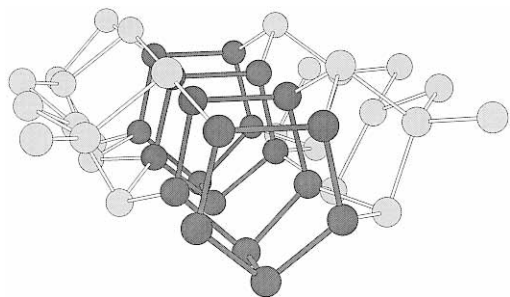


Figure 3. Tin atoms in the A area in Figure 2 highlighted to show both the pentagonal clusters and their interconnections via pentagons in B (light gray).

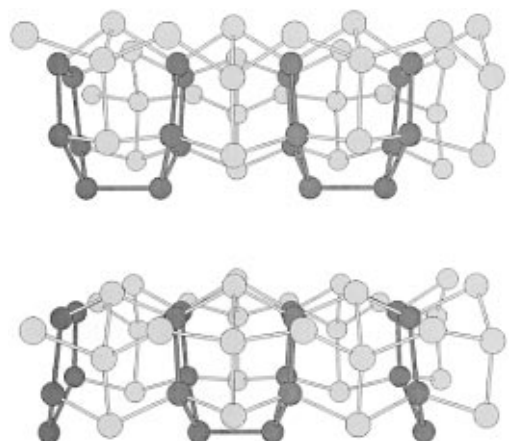


Figure 4. An adjoining pair of A, B columns viewed roughly along \bar{c} . This view retains the highlighted pentagons from Figure 3 and shows their relationship to one another from chain to chain along the vertical b axis.

In the first, direct bonds between the 3b-Sn apices at the bottom of the central pentagon alternate with 6.00-Å-long contacts along the a axis, as shown close up in a slightly different view in Figure 3. A normal [001] view in Figure 4 illustrates that this bonding arrangement also alternates along the b axis between adjoining columns of stacked pentagons so that two apices bonded in one pentagonal column are not bonded in adjoining columns and vice versa. The second connection of these A columns is through a parallel series of edge-bridging pentagons B (Figure 2) that also run along the a axis. These contain three 4b-Sn atoms and two 3b-Sn atoms and are shown in lighter shading in Figure 3. This ordering results in the doubling of the unit cell in both the a and b directions.

The central A,B clusters of pentagons are further connected in the a - c plane by single bonds to another series of stacked pentagons labeled "C" in Figure 2, and these connect directly into the empty central 9-ring "D". These two fragments are highlighted in Figure 5. As with the series of tin pentagons (A) that stack along the a axis, bonds between the C pentagons at the apices (which project into the cation channel) also alternate in this direction with long and short separations. However, the arrangement of bonds along \bar{c} between the 3b-Sn here are opposite to that in the other (A) pentagon stack such that when one pentagonal stack is bonded, the other is not.

The overall alignment of these pentagonal tin subunits and D rings along the b direction results in the formation of large banana-shaped channels. All of the sodium countercations are found either in these or in the A and C columns. As might be expected from electrostatic arguments, the edges of these channels are nearly all defined by 3b-Sn⁻ atoms, and the sodium cations are closest in proximity to the charged tin atoms rather than the formally neutral 4b-Sn. The doubling of the c axis in

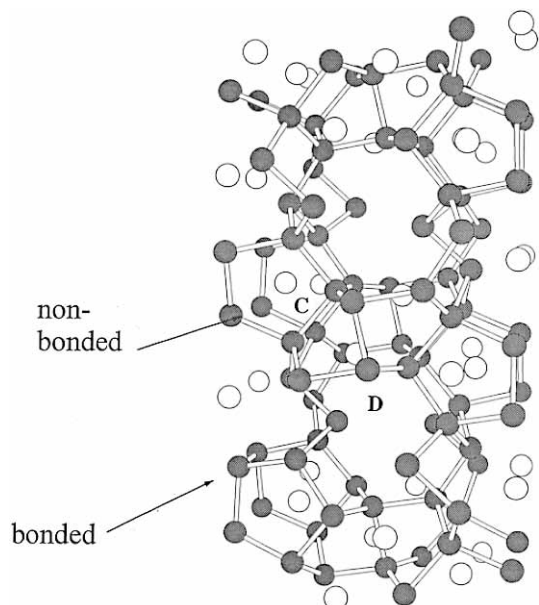


Figure 5. A segment of the structure highlighting the tin atoms in two central rings D and the four adjoining pentagonal stacks C (Figure 2). The alternation along \bar{a} of bonded and nonbonded interactions between the projecting 3b-Sn atoms in ring C is marked.

the compound to approximately 51 Å reflects the banana-shaped channels and their ordering and orientation within the unit cell. The smaller open D channels through the center of the cell are lined mainly by neutral tin atoms, but for a central belt of three 3b-Sn₇ atoms (Figure 2). However, these would provide a very poor environment for sodium cations, so the D channel is left empty.

One of the more intriguing questions about Na₅Sn₁₃ and the separation of 3b- and 4b-Sn is the Sn-Sn distance that should be considered nonbonding. The Sn-Sn bond distances in this compound are easily segregated into two types, those at 2.80–2.98 Å and those around 4 Å. There is only one distance in the middle, a Sn11-Sn11 contact in the D ring at 3.61 Å. If this represents a bond, then the Sn11 atoms have tetrahedral coordination, while if the distance is too long, then these are both 3b-Sn with a lone pair of electrons pointing more or less at each other. Extended Hückel molecular orbital (band) calculations were carried out in order to address this question. Overlap populations for each of the three bond distance groups show that the typical overlap populations for ~2.9 Å bonds is 0.46 and the 3.6 Å Sn11-Sn11 bond has a significant positive overlap population of 0.26, while all more distant interactions display nonpositive populations, indicative of no bond formation. Inclusion of the 3.6 Å Sn11-Sn11 bond makes Na₅Sn₁₃ closed-shell; that is, the numbers of 3b-Sn⁻ and Na⁺ are equal. The contrast with conventional metallic bond length-bond order relationships, which would fall off by a factor of 12 here, is notable but scarcely surprising in view of the obviously directional bonding.

Magnetic measurements on Na₅Sn₁₃ show it to be diamagnetic. The uncorrected data have a small (and not uncommon) paramagnetic tail that changes the net signal to positive below about 20 K. Although this event would not change the conclusions, the tail was well fit as an $S = 1/2$ system, and the impurity contribution was subtracted from the data (Experimental Section). Both data sets are shown in Figure 6. Even though it is a very complex structure with 208 tin atoms in the unit cell, the compound is electron precise, Na⁺₈₀(Sn⁻₈₀)(Sn⁰₁₂₈), according to both simple Zintl-Klemm formalisms and its diamagnetic behavior.

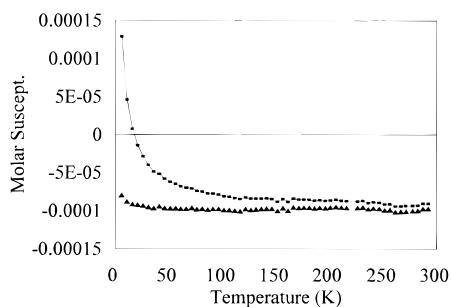


Figure 6. Magnetic susceptibility of $\text{Na}_5\text{Sn}_{13}$ at 3 T. The top and bottom plots show the data before and after correction for a paramagnetic impurity. In both cases, the data indicate a diamagnetic compound.

Compared with other polar intermetallic alkali-metal–tin phases reported to date, the new compound $\text{Na}_5\text{Sn}_{13}$ exhibits a new structural type in that the main building blocks are clusters built of simple tin pentagons. The last units are also components of the pentagonal dodecahedra that appear in K_8Sn_{25} .⁸ Although the structure of $\text{Li}_7\text{Ge}_{12}$ has not been fully reported in the literature, general ideas about its structure published in review articles¹⁸ show that it too consists of layers built of stacked

pentagonal units as $\text{Na}_5\text{Sn}_{13}$ although connected in a simpler manner and with a smaller unit cell to accommodate the different framework charges. The present structure is especially remarkable for the complexity that is necessary to fill space well and to conform precisely to the Zintl–Klemm electron-counting formalisms, yet it also further highlights the very simplicity of these valuable guidelines. These rules of course never predict a structure, but they are very useful guidelines for ratifying the plausibility of a new structural result.

Acknowledgment. The authors thank Dr. Leonard Thomas for maintenance of the single-crystal X-ray diffraction facility at Iowa State University.

Supporting Information Available: An illustration with the atom-numbering scheme (1 page). Listings of crystallographic details and atom displacement parameters, in CIF format, are available on the Internet only. Ordering and access information is given on any current masthead page.

IC9703181

- (18) (a) Gruttner, A.; Nesper, R.; von Schnering, H.-G. *Acta Crystallogr.* **1981**, 37A, C161. (b) Nesper, R. *Prog. Solid State Chem.* **1990**, 20, 1.